Building and Environment 296 (2026) 114471

Contents lists available at ScienceDirect

Building and Environment

journal homepage: www.elsevier.com/locate/buildenv

Beyond summer cooling: Evaluating winter thermal performance of urban trees in subtropical coastal region

Lingye Yao [a], Kevin Lau [b], Xiang Zhang [c], Zhixin Liu [d], Genyu Xu [e], Kai Gao [f,*], Mohammad A. Rahman [g], Edward Ng [a]

[a] School of Architecture, The Chinese University of Hong Kong, Hong Kong, China
[b] Department of Civil, Environmental and Natural Resources Engineering, Luleå University of Technology, Luleå, Sweden
[c] Chair for Strategic Landscape Planning and Management, Technical University of Munich, Freising, Germany
[d] School of Architecture and Landscape, The University of Sheffield, Sheffield, UK
[e] School of Architecture and Planning, Yunnan University, Kunming, China
[f] School of Property, Construction and Project Management, Royal Melbourne Institute of Technology, Melbourne, Australia
[g] School of Agriculture, Food and Ecosystem Sciences, The University of Melbourne, Burnley, Victoria 3121, Australia

ARTICLE INFO

Keywords:
Outdoor thermal comfort (OTC)
Street canyon
ENVI-met
Subtropical winter
PET
UTCI

ABSTRACT

Urban trees are widely recognized as effective nature-based solutions for urban heat mitigation, yet current design strategies focus predominantly on optimizing summer cooling, leaving their potential for winter thermal regulation understudied. This oversight raises a critical question: Do tree configurations optimized for summer cooling remain thermally beneficial in winter? To address this issue, this study conducted a parametric analysis using ENVI-met to evaluate the seasonal thermal performance of urban trees in subtropical coastal city Hong Kong under extreme summer and winter conditions. Multi-scenario simulations were run, incorporating eight urban canyons characterized by discrete sky view factors (SVF=0.1–0.8) based on typical morphological categories, two street orientations (N-S, E-W), and two tree species (evergreen *Ficus microcarpa*, deciduous *Lagerstroemia speciose*). Results indicate that both evergreen and deciduous trees provided comparable cooling in summer, with mean differences of 0.21 °C in PET and 0.35 °C in UTCI. A consistent peak cooling of up to 8 °C in PET and 5 °C in UTCI was observed at SVF = 0.7 for both species. In winter, evergreen trees improved comfort by wind shielding in deep, low-SVF canyons (up to 1 °C in PET; 6 °C in UTCI), while deciduous trees enhanced comfort through solar access in shallow, high-SVF canyons (over 0.3 °C PET; 1 °C in UTCI). For subtropical coastal contexts, our findings suggest that tree selection and placement should be seasonally adaptive. This study provides a methodological framework and preliminary insights for climate-adaptive planting strategies in urban canyons from a year-round perspective.

1. Introduction

1.1. Trees as Nature-based Solutions for urban heat mitigation

The escalating impacts of global warming and climate change are intensifying urban overheating, posing significant challenges to human health and energy sustainability [1–3]. Urban green infrastructure (GI) has been recognized and increasingly implemented as an efficient design strategy to mitigate urban heat [4–7], owing to its nature-based mechanisms and cost-efficient cooling potentials [8]. Ground trees, green roofs, and green walls (also referred to as green façades or vertical greenings) are three widely implemented GI typologies [9–11]. Among these, trees have been identified as the most effective in moderating pedestrian-level thermal comfort [12,13], through shade provision, evapotranspiration, and airflow regulation [14–16]. Empirical studies underscore the superior cooling performance of trees compared to other GI typologies (e.g., green roofs and walls). For instance, field measurements in subtropical Hong Kong demonstrate that trees can reduce pedestrian-height air temperature by up to 4 °C and mean radiant temperature (MRT) by 16 °C during summer, outperforming alternative GI solutions [10]. This aligns with global meta-analyses indicating that tree-based interventions effectively lower peak temperatures below 26 °C in 83 % of 110 cities across 17 climate zones [17].

However, the efficacy of urban trees is highly context-dependent, influenced by four key factors: (1) background climate conditions, (2)

* Corresponding author.
E-mail address: kai.gao@rmit.edu.au (K. Gao).

https://doi.org/10.1016/j.buildenv.2026.114471
Received 18 September 2025; Received in revised form 20 February 2026; Accepted 9 March 2026
Available online 10 March 2026
0360-1323/© 2026 The Author(s). Published by Elsevier Ltd. This is an open access article under the CC BY license (http://creativecommons.org/licenses/by/4.0/).

Nomenclatures

CFD	Computational Fluid Dynamics
EBM	Energy Balance-based Model
FM	*Ficus microcarpa*
GI	Green Infrastructure
H/W	Aspect ratio, building height/canyon width
HKO	Hong Kong Observatory
LAD	Leaf area density (m^2/m^3)
LAI	Leaf area index (m^2/m^2)
LS	*Lagerstroemia speciose*
MRT	Mean Radiant Temperature (°C)
PET	Physiological Equivalent Temperature (°C)
RH	Relative humidity (%)
R^2	Coefficient of determination
RMSE	Root mean square error
SLF	Seasonal leaf factor
SR	Global solar radiation (W/m^2)
SVF	Sky View Factor
T_a	Air temperature (°C)
UTCI	Universal Thermal Climate Index (°C)
WS	Wind speed (m/s)

urban morphological characteristics, (3) species-specific tree traits, and (4) planting design strategies [17,18], which underscores the need for site-specific design guidelines to optimize their thermal benefits.

1.2. Seasonal dynamics of tree effects and the need for winter assessment

While the summer cooling benefits of urban trees are well-documented, their winter performance remains understudied [19], particularly in hot regions [20]. Trade-offs between wind shielding and solar access are critical for winter outdoor thermal comfort yet overlooked. For instance, evergreen trees may improve winter thermal comfort by blocking wind to reduce wind chill in urban canyons but simultaneously limit desirable solar penetration. Conversely, deciduous trees allow greater solar access in winter due to leafless canopies but offer less wind protection.

Regional studies highlight these trade-offs; though limited literature is available for winter conditions (Table A in Appendix A). In tropical Singapore, evergreen trees provide year-round cooling [21], whereas in hot-summer and cold-winter regions they can worsen cold stress by blocking sunlight, with a reported reduction of 3.6 °C in physiological equivalent temperature (PET) [19]. In cold-winter cities like Lhasa, deciduous trees enhance winter thermal comfort through solar access, with PET increased by up to 10.6 °C [22]. Subtropical coastal cities like Hong Kong present unique challenges in winter, where strong winds may compromise pedestrian comfort [23,24]. In such contexts, wind control is a key factor in winter urban tree planning, yet the trade-off between wind-sheltering effect of evergreen trees and solar access provided by deciduous trees remains largely unexplored. Addressing this gap is essential for developing climate-resilient urban landscapes that balance seasonal thermal demands in these regions from the year-round perspective.

1.3. Impacts of urban morphology on tree effects

In addition to climate background and tree species, urban morphology is another significant factor influencing tree effects [25]. The urban canyon (or street canyon), a fundamental basic geometric unit of cities, plays a particularly important role. Its geometry, for which the sky view factor (SVF) serves as a holistic indicator of openness, is a well-documented critical driver of microclimate and outdoor thermal comfort [26,27]. SVF is defined as the proportion of visible sky from a point within the canyon [28]. It represents the ratio of the radiation received by a planar surface to that from the entire hemispheric environment, ranging from 0 to 1. A value of 0 indicates that all outgoing radiation is blocked by obstacles while a value of 1 means that all radiation propagates freely into the sky without any obstruction [29]. Following SVF-based literature [30,31], we adopt three classification levels: Low-SVF (SVF$<$0.3) for dense spaces, Moderate-SVF (0.3$\leq$SVF$<$0.7) for moderately dense spaces, and High-SVF (SVF$\geq$0.7) for open spaces. This indicator governs solar access and radiative heat exchange within canyons. For instance, deeper canyons with lower SVF exhibit reduced daytime temperatures due to building shading but experience higher nighttime heat retention, potentially complementing or counteracting tree effects. Trees in low-SVF canyons (where building shadows dominate) demonstrate weaker daytime cooling (ΔMRT=21°C) compared to high-SVF canyons (ΔMRT=26°C) evidenced by summer field measurements [32]. Furthermore, a parametric study promotes a morphology-based tree selection strategy tailored to low-, moderate-, and high-SVF canyons based in hot summer conditions [33]. However, existing research predominantly focuses on hot summer conditions, neglecting seasonal interactions between tree species and canyon geometry.

1.4. Numerical approaches to understanding tree effects in urban canyons

Research on tree-canyon interactions employs field measurements [32,34], wind tunnel tests [35,36], and numerical simulations [33,37,38]. Among these, numerical modeling has become a primary method due to advances in computational power, enabling systematic analysis of the complex parametric space defined by climate, morphology, and tree characteristics. For urban greenery simulation, two key modeling families are commonly used [39]: Energy balance-based models (EBM) such as SUEWS, RayMan, and SOLWEIG, and Computational Fluid Dynamics (CFD)-based models such as OpenFOAM, urbanMicroclimateFoam [38,40], Fluent, Phoenics, and ENVI-met.

Compared to EBM tools, CFD-based models enable coupled simulations of fluid dynamics, heat transfer, and radiative exchange within urban canyons at higher resolution. This capability has made them widely applicable in urban canyon studies. Concerning vegetation parameterization, ENVI-met stands out among CFD-based tools for its advanced and detailed representation of vegetation [41]. It corporates dedicated modules for various greenery types, including simple plants for grass and hedges, green roof/façade module for building envelope greening, 3D-plants, and Lindenmayer-Systems-based trees [42], and also integrates these with a detailed solver for in-canyon radiation exchange. This makes ENVI-met a particularly suitable and powerful tool for investigating tree effects within complex built environments.

1.5. Research gaps and objectives

Despite extensive research on urban trees as heat mitigation tools, critical knowledge gaps persist.

- While the summer cooling benefits of urban trees are well-documented, their holistic thermal performance across seasons is insufficiently studied, especially in winter. The trade-offs between wind shelter (reducing convective heat loss) and solar access (enhancing radiant gain) remain unexamined in winter.
- Existing research often evaluates tree species in isolation or focuses solely on evergreen trees in fixed urban settings. A comprehensive understanding of how evergreen and deciduous trees interact with different urban geometries across seasons in lacking, limiting context-specific design strategies.
- Although tree efficacy is known to depend on climate, urban morphology, species traits, and planting strategies, practical guidelines that integrate these factors are absent, particularly for

subtropical coastal cities with unique winter wind exposure. A "right tree, right place, right time" framework that balances summer cooling and winter warming is urgently needed to translate theoretical research into climate-adaptive design practice.

To address these gaps, this study evaluates the seasonal effects of urban trees using ENVI-met simulations. We assess urban canyons with eight SVFs, two street orientations, and two tree species (evergreen/deciduous) during summer and winter in Hong Kong. This approach significantly advances existing ENVI-met-based tree studies by moving beyond a summer-only focus, to provide an explicit, systematic comparison of seasonal trade-offs in a subtropical coastal context. By integrating a comprehensive parametric analysis of urban morphology (via SVF and orientation) with a comparison of evergreen and deciduous species, this study aims to provide actionable, site-specific, seasonally-aware tree design guidelines that are currently absent for subtropical coastal cities like Hong Kong.

2. Materials and methods

The workflow of this study is outlined in Fig. 1. First, building upon the previous research work of the authors' team [33], a framework of "right tree, right place, right time" was proposed, incorporating urban geometry, urban tree species, and season. Second, guided by these three key factors, microclimate model ENVI-met was employed to simulate 16 idealized urban canyons, characterized by combinations of 8 SVF classes (0.1–0.8) and 2 street orientations (N-S, E-W). Each canyon model was assigned 2 greening schemes—evergreen tree (*Ficus microcarpa*, FM) and deciduous tree (*Lagerstroemia speciose*, LS), alongside a "Notree" baseline, resulting in a total of 96 scenarios simulated during 2 seasons. Third, the output data, including air temperature (T_a), relative humidity (*RH*), wind speed (*WS*), and *MRT*, were extracted for microclimate assessment. Additionally, PET and UTCI, computed by BIO-met module, enabled a detailed seasonal analysis of thermal comfort. Finally, actionable tree design guidance was derived, tailored to subtropical coastal cities from a year-round perspective.

2.1. Study area and climatic background

Hong Kong (22°08'N–22°35'N, 113°49'E–114°31'E), a typical subtropical coastal city on the southern coast of China, experiences a humid subtropical climate (Cwa) under the Köppen-Geiger classification [43]. The city is characterized by prolonged hot seasons and relatively short cold periods, which has led to a predominant research focus on the heat mitigation benefits of urban greenery during hot periods. Long-term climatic records (Fig. 2) from the Hong Kong Observatory (HKO) [44] show that, in summer season (May to Sept), daily temperatures typically range from around 26 °C to above 31°C, while during winter months (Dec to Feb), temperatures typically average between 15 °C and 19°C, occasionally interrupted by cold fronts accompanied by dry northerly winds [23]. The monthly mean RH fluctuates between 70 % and 80 % throughout the year, and solar radiation peaks at nearly 800 W/m^2 in summer.

Wind regime in Hong Kong is strongly influenced by the East Asian Monsoon system, resulting in distinctly seasonal prevailing wind patterns. In summer, winds predominantly originate from the south to southeast, bringing warm, moist maritime air from the South China Sea under the influence of the southwest monsoon. Conversely, winter is characterized by prevailing northeasterly winds that convey cooler and drier continental air masses, driven by the northeast monsoon. Notably,

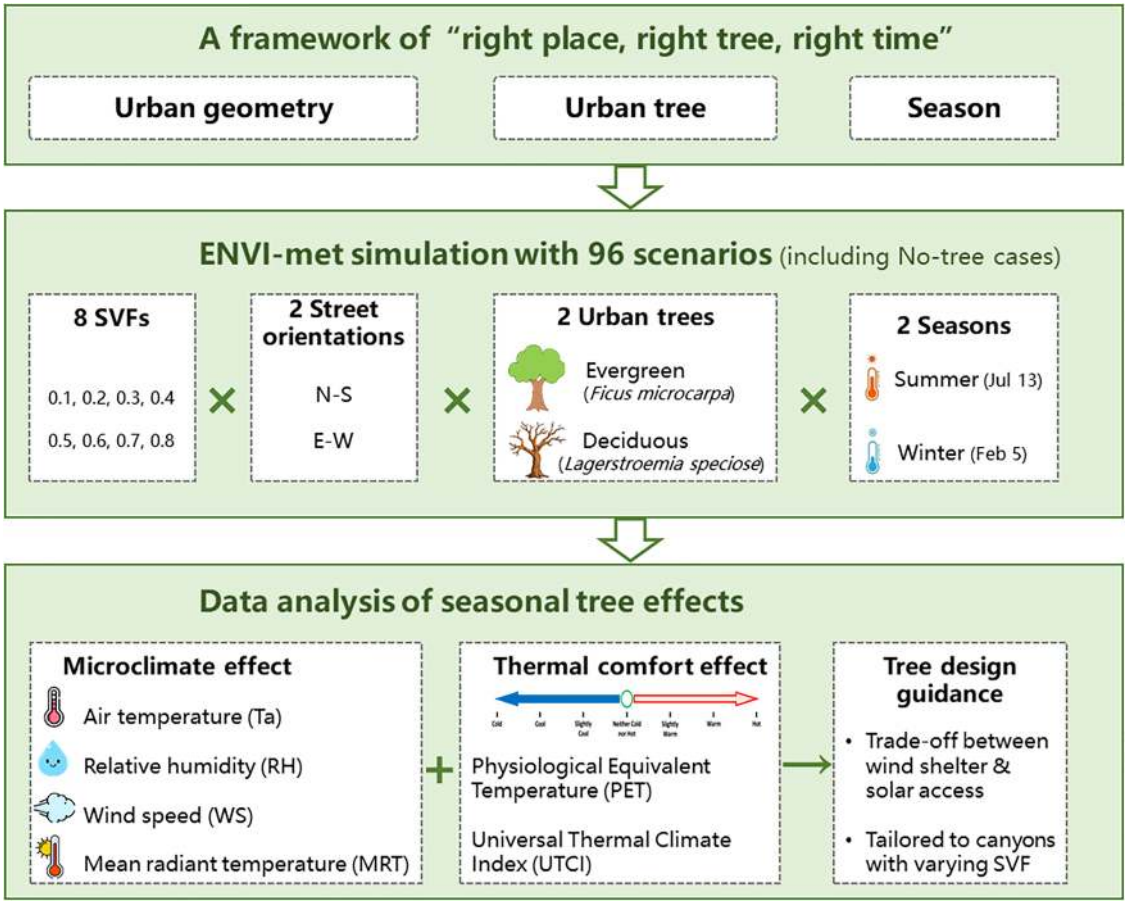


Fig. 1. Research framework of this study.

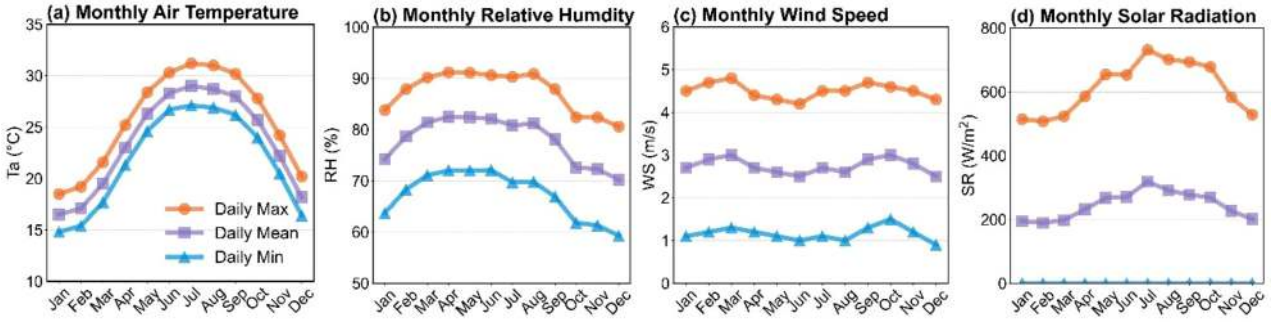


Fig. 2. Monthly means of daily maximum, mean, and minimum (a) air temperature, (b) relative humidity, (c) wind speed recorded at the Hong Kong Observatory (HKO) station, and (d) global solar radiation recorded at King's Park between 1991–2020. (Source: [44]).

wind speeds tend to be higher in winter than in summer (Fig. 2c), with occasional cold surges producing sustained wind speed up to 16.7 m/s in urban areas [23]. These climatic backgrounds are essential considerations for sustainable climate-adaptive urban design [45].

2.2. Summer/winter day selection and meteorological characteristics

Selecting representative meteorological conditions is crucial for reliable microclimate simulations [46]. To ensure the results reflect typical seasonal extremes, we selected the hottest (13 July 2015) and coldest (5 February 2018) days, based on daily mean temperature, from a 2010–2020 dataset, obtained from the Hong Kong Observatory (HKO) station located in the downtown of Hong Kong (22°18′07"N, 114°10′27"E; https://www.hko.gov.hk/en/cis/stn.htm), for summer and winter scenario simulations. To isolate the thermal effects of tree configurations from wind variability, this study employed constant wind speeds (set to daily averages) and preserved the prevailing wind directions (180° in summer and 0° in winter, which are parallel to urban canyons) throughout all simulation hours. Key input meteorological parameters, including T_a, *RH*, *WS*, and global solar radiation (*SR*), are presented in Fig. 3, with statistical characteristics summarized in Table 1 and detailed hourly data provided in Tables B1 and B2 of Appendix B.

Table 1
Statistical summary of key meteorological parameters for the selected summer/winter days.

Parameter	Season	Max	Min	Mean	Median
T_a	Summer	37.1	30.0	32.4	31.0
(°C)	Winter	12.5	4.4	8.4	8.2
RH	Summer	83.9	40.5	63.5	69.3
(%)	Winter	35.6	13.4	25.4	28.3
WS	Summer	3.0	0.1	1.8	1.8
(m/s)	Winter	4.5	2.6	3.9	4.0
SR	Summer	970	0	273	48
(W/m^2)	Winter	761	0	186	0

2.3. ENVI-met selection and model overview

ENVI-met, a three-dimensional microclimate model based on CFD and thermodynamics, was employed for this parametric study. ENVI-met was chosen for its proven capability to simulate the coupled

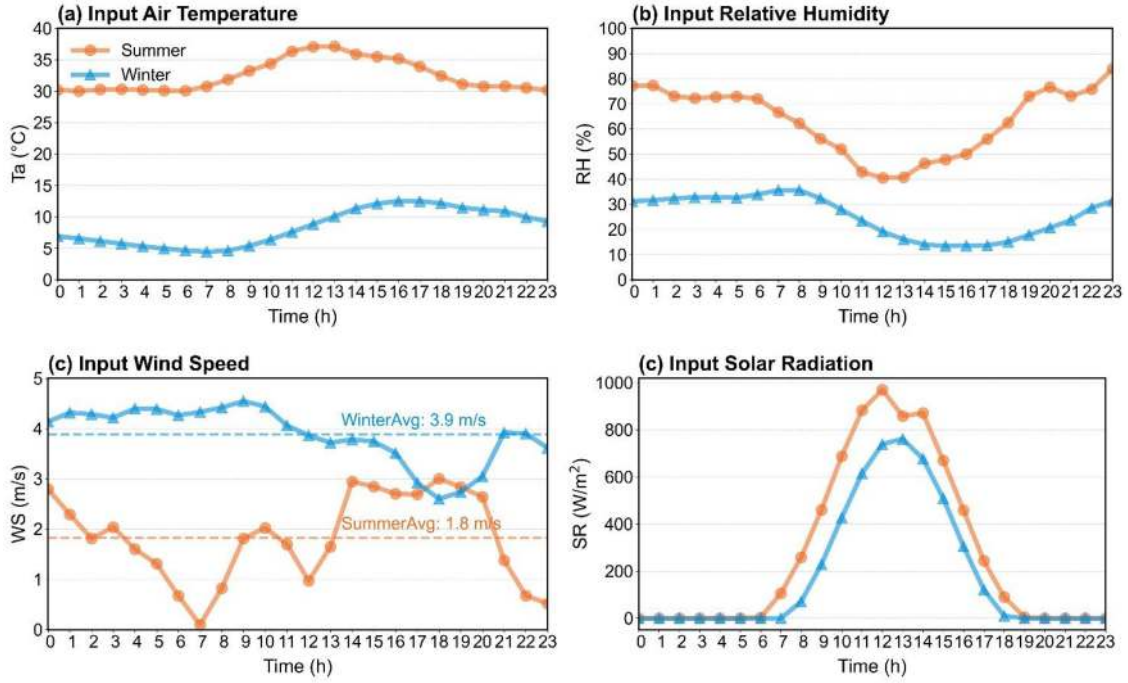


Fig. 3. Diurnal variations of key input meteorological parameters for the selected summer (13 Jul 2015) and winter (5 Feb 2018) days: (a) air temperature (T_a), (b) relative humidity (*RH*), (c) wind speed (*WS*, wind averages were used as the inputs), and (d) global solar radiation (*SR*). (Data source: HKO station; https://www.hko.gov.hk/en/cis/stn.htm).

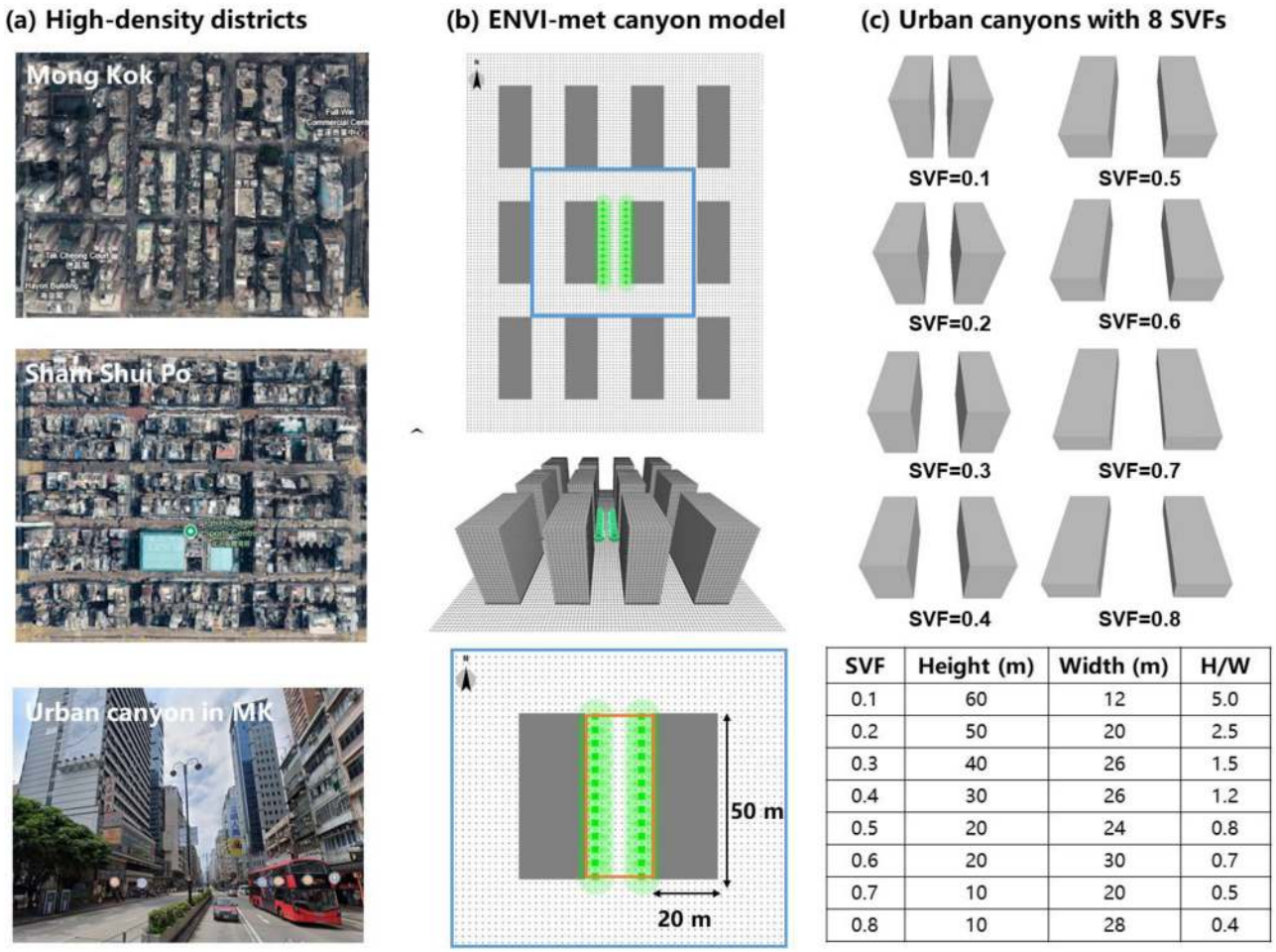
interactions between urban geometry, vegetation, and radiative exchange at the pedestrian level [8], which align with our research questions. It can compute the surface energy fluxes among buildings, vegetation, soil, and the atmosphere. The latest version (v5.8.0) offers improved features for tree modeling, including detailed 3D tree geometry, advanced soil and root models, and the TreePass module for assessing wind risks and growth conditions [47], which helps better understand street tree effects in urban environments. For a detailed description of ENVI-met model architecture, including the atmospheric, soil, vegetation, and building models, as well as its discretization scheme and numerical methods, readers are referred to the technical documents [42].

ENVI-met has been widely validated for simulating urban greenery and its microclimatic impacts [8,48–50]. Specifically, its performance has been confirmed for modeling urban street trees in Hong Kong's hot summer climate through previous validation work by the authors [12,33,34], and its applicability has also been demonstrated in subtropical cold environment, such as winter conditions in Shanghai, China [51]. It is also important to acknowledge the limitations of ENVI-met, including grid-dependency [52] and potential biases in thermal fields and comfort indices [53]. To address these issues, the present study incorporates the following mitigation strategies: (1) a mesh sensitivity analysis to ensure grid-independent results for key variables (Appendix C); and (2) the application of established, localized parameterizations for materials and vegetation (Section 2.4.2 & 2.4.3).

2.4. Parametric study design

2.4.1. Generic urban canyon model

The generic urban canyon models were simplified from prototypes in the high-density districts of Mong Kok and Sham Shui Po in Hong Kong (Fig. 4a), ensuring their representativeness of the prevalent urban morphology of this city. Each canyon model consists of two parallel rows of building groups (50 m × 20 m), with building heights varying from 10 to 60 m to achieve different SVF scenarios. To account for the influence of surrounding buildings, the model also includes 10 neighboring buildings, identical in form to the central ones, as illustrated in Fig. 4b. This simplified model, established and validated in our previous work [12,54], captures the essential urban morphology while providing a controlled environment for focused analysis. Following Oke's estimation method [55] and the typical morphological categories used in previous research [12,33,54], eight SVF scenarios were generated by adjusting the building height / street width (H/W) combination. These SVF classes, ranging from 0.1 to 0.8, represent a comprehensive spectrum of urban forms in Hong Kong. The corresponding H/W ratio for each SVF threshold and their geometries are provided in Fig. 4c. Morphologically, these values span from deep urban canyons (e.g., SVF=0.1, characteristics of dense cores) to wide, open streets (e.g., SVF=0.8, like boulevards or parkways), with intermediate values representing medium-depth canyons typical of mixed-use areas.



SVF	Height (m)	Width (m)	H/W
0.1	60	12	5.0
0.2	50	20	2.5
0.3	40	26	1.5
0.4	30	26	1.2
0.5	20	24	0.8
0.6	20	30	0.7
0.7	10	20	0.5
0.8	10	28	0.4

Fig. 4. Illustration of generic urban canyon model parameterization: (a) prototype of typical neighborhood and urban canyons in Mong Kok & Sham Shui Po, Hong Kong (Source: Google Earth), (b) idealized neighborhood model with generic urban canyons (focused central canyon marked in blue, analysis zone marked in orange) and 3D view model domain with mesh in ENVI-met, and (c) urban canyon models with 8 SVF classes and the corresponding table.

2.4.2. Tree selection and settings

Ficus microcarpa (FM) and *Lagerstroemia speciose* (LS) were selected as the representative evergreen and deciduous species, respectively. These trees are characterized by large crowns and dense canopies (Table 2), which are effective for shading and wind shelter. Both species rank among the top 20 most common urban trees in Hong Kong's Street Tree Selection Guide [56] and are also prevalent in subtropical South China cities [41]. Moreover, these two species are planted within the urban canyons of the investigated districts. Key morphological and thermo-physical parameters and model settings for these two species are detailed in Table 2. Trees were planted in a line along the streets at intervals of 2 m, as illustrated in Fig. 4b.

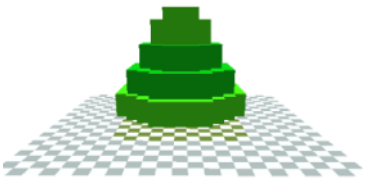
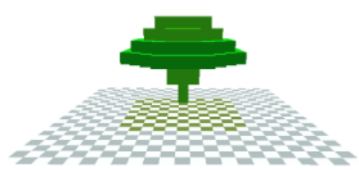
To standardize the comparison and control variables, both trees were set to the same height and crown diameter. The values for tree height, crown diameter, and bole height were sourced with approximation from the ENVI-met tree model library specific to subtropical vegetation, which was developed by [41] based on extensive review of previous field measurements and ENVI-met greenery studies. The values of leaf albedo and LAI (Leaf Area Index) were also referenced from this library. LAD (Leaf Area Density) at each height level was calculated from LAI using the following empirical formula developed by Lalic and Mihailovic [58]:

$$LAD(z) = LAD_{\max}\left(\frac{H - z_{\max}}{H - z}\right)^{n} \exp\left[n\left(1 - \frac{H - z_{\max}}{H - z}\right)\right] \tag{1}$$

$$LAI = \int_{0}^{H} LAD_{\max}\left(\frac{H - z_{\max}}{H - z}\right)^{n} \exp\left[n\left(1 - \frac{H - z_{\max}}{H - z}\right)\right] dz \tag{2}$$

$$\begin{cases} n = 6, 0 \le z < z_{\max} \\ n = 0.5, z_{\max} \le z \le H \end{cases}$$

Table 2
Main parameters and specifications for tree model in ENVI-met.

Type	Item	Evergreen	Deciduous
Tree species	Name	*Ficus microcarpa* (FM)	*Lagerstroemia speciose* (LS)
	Native/Exotic	Native	Exotic
Tree physical trait	Height (m)	10	10
	Crown diameter (m)	11	11
	Bole height (m)	1.3	1.5
Microclimate-sensitive modeling parameters	Foliage albedo [a]	0.31	0.31
	Foliage transmittance	0.1	0.3
	Foliage emissivity	0.96	0.96
	LAI (m^2/m^2) [b]	3.88	3
	LAD (m^2/m^3) [c]		
	At 1 m	–	–
	At 2 m	0.3253	0.1613
	At 3 m	0.4243	0.2341
	At 4 m	0.5237	0.3334
	At 5 m	0.5753	0.4473
	At 6 m	0.5676	0.5139
	At 7 m	0.5322	0.5023
	At 8 m	0.4297	0.4408
	At 9 m	0.1741	0.2293
	At 10 m	–	–
	Tree calendar	SLF [d] =1.0	Summer: SLF=1.0 (leaf-on) Winter: SLF=0.2 (leaf-off)
Typical photograph	Front view		
ENVI-met model	Front view		

[a] Foliage albedo: The value of 0.31 is sourced from [41,48].
[b] LAI: The value of 3.88 is sourced from [41,48], and value of 3 from [41,57].
[c] LAD: The LAD value at each height level was calculated using the empirical relationship by Lalic and Mihailovic [58].
[d] SLF: Seasonal leaf factor.

Where LAD (z) is the leaf area density at the height of z within the canopy (m^2/m^3), LAD_{max} is the maximum leaf area density at z_{max} (m^2/m^3), H is tree height (m), LAI is the leaf area index (m^2/m^2), n is the empirical constant. z_{max} is set to 5 m and 6 m for *Ficus microcarpa* and *Lagerstroemia speciose* respectively based on field surveys of Hong Kong local street trees.

The Tree Calendar in ENVI-met is a dynamic module that simulates phenological changes in vegetation, including leaf growth and shedding, to accurately represent seasonal variations in biometeorological processes [47]. It incorporates the Seasonal Leaf Factor (SLF), a dimensionless parameter ranging from 0 (leafless) to 1 (full foliage), modulating LAD over time. This factor affects shading, transpiration, and turbulence patterns. In this study, SLF values were maintained constant at 1.0 for evergreen (FM), while for deciduous (LS), values were set to 1.0 in summer and 0.2 in winter, respectively. However, it should be noted that the simplified representation of phenology via SLF may introduce uncertainties in OTC assessments, particularly in winter radiative and latent heat exchanges.

2.4.3. Model configurations and scenario design

Generic urban canyon models with 20 m boundary spaces and 10 nesting grids were developed in ENVI-met for different SVF scenarios, employing a grid resolution of 2 m. A mesh sensitivity analysis was conducted as detailed in Appendix C. The analysis showed no significant variations (<5 %) in key output metrics across grid resolutions of 2 m, 1.5 m, and 1 m. Therefore, the 2 m grid was considered sufficiently accurate for the scope of this study. The domain was discretized using an orthogonal Arakawa C-grid. Simulations were run from 0:00 to 23:00 in full-forcing mode, driven by the user-defined meteorological boundary conditions for the selected summer and winter days (see Section 2.2), including air temperature, relative humidity, direct/diffuse shortwave radiation, longwave radiation, wind speed/direction, and precipitation, with full hourly data provided in Tables B1 and B2 in Appendix B. A fixed time step of 2 s was used. A spin-up period of 24 h was performed prior to the analysis period to minimize the influence of initial conditions.

For materials and surfaces, we applied representative thermophysical values to reflect typical urban conditions. The building walls were modeled as heavy concrete with cement, the roof as concrete tile, and the ground surface as concrete pavement. The material properties were the average of these component materials. The chosen values were adopted from the building envelope database [59] and previous observational and validation studies [60–62]. Detailed specifications for material properties can be found in Table D, Appendix D. Tree models for evergreen (FM) and deciduous (LS) were created using the Albero module, with main parameters specified in Table 2. Key parameters for model configurations are listed in Table 3.

The scenario design for parametric studies can be found in Table E of Appendix E. This study combines 8 urban canyons configurations (varying by SVF), 3 greening schemes (evergreen, deciduous, Notree), and 2 street orientations (N-S, E-W), resulting in 96 simulation runs across summer and winter seasons.

Table 3
ENVI-met model configurations.

Category	Item	Specification
Grid settings	Domain size	Scenario-specific
	Building size	20 m × 50 m
	Grid resolution	2 m × 2 m × 2 m
	Vertical grid generation	Telescoping factor: 20 % Start telescoping after height: building height
	Nesting grids	10
Simulation time	Date	Summer: Jul 13; Winter: Feb 5
	Time	0:00–23:00
Meteorological boundary conditions	Scheme	Full forcing
	Hourly inputs	Hourly direct/diffuse shortwave radiation, air temperature, relative humidity, wind speed, wind direction, precipitation (Section 2.2, Tables B1 and B2 in Appendix B)
	Site roughness	0.20
Soil settings	Temperature and humidity profiles	Observations from field measurements [60]
Building	Wall	Heavy concrete with cement (Table D in Appendix D)
	Roof	Concrete tile (Table D)
Soil and surface	Ground	Concrete pavement (Table D)
Vegetation	Tree	Evergreen: *Ficus microcarpa* [FM] (Table 2) Deciduous: *Lagerstroemia speciose* [LS] (Table 2)

2.5. Methods of data analysis

2.5.1. Assessment indicators

The outputs of T_a, *RH, WS*, and *MRT* were extracted as microclimatic indicators. For outdoor thermal comfort (OTC) assessment, both the Physiological Equivalent Temperature (PET) and Universal Thermal Climate Index (UTCI) were employed. This dual-index approach was adopted to provide a more robust and mechanistically detailed analysis. While both indices are well-validated and widely used in outdoor thermal comfort studies [63–65], and both incorporate key meteorological and human physiological parameters for a holistic assessment, they exhibit different sensitivities to key meteorological parameters. Specifically, according to the literature, PET demonstrates greater sensitivity to variations in radiant temperature, making it a strong indicator for assessing the impact of shading from trees and buildings [66]. In contrast, UTCI is more sensitive to changes in wind speed and humidity, thereby better capturing the effects of ventilation and evaporative cooling [67]. By utilizing both indices, this study aims to not only characterize thermal comfort levels but also elucidate the dominant physical processes—whether radiative or convective-driven—through which street trees modify the microclimate. This comparative analysis is conducted for both summer and winter to determine if the relative performance and interpretation of these indices change with seasonal weather patterns.

PET and UTCI were calculated using the BIO-met module of ENVI-met. Biometeorological values for a 35 y-old male adult (75 kg, 1.75 m) with slow-walking activity (1.34 m/s) were applied. Clothing insulation was set at 0.3 clo for summer [65] and 0.9 clo for winter to align with subtropical conditions. Tree effects were quantified by the differences between the tree-planting scenario and Notree scenario:

$$\Delta V(x_i, y_i) = V_{Tree}(x_i, y_i) - V_{NoTree}(x_i, y_i) \quad (3)$$

Where $V(x_i, y_i)$ is the variable (T_a, *RH, WS, MRT*, PET, UTCI) at grid cell (x_i, y_i). Negative values represent cooling effects while positive values indicate warming effects.

2.5.2. Analysis domain and temporal period

To avoid model boundary effects and to better capture the microclimate impact of street trees on roadside pedestrian spaces, the analysis was confined to the central urban canyon zone, i.e. the core space between the surrounding buildings (as delineated by the orange rectangle in Fig. 4b) at a pedestrian-level height of 1.4 m (dz=3). Model outputs were then evaluated over a diurnal cycle (0:00–23:00) following the spin-up period. A daytime period from 07:00 to 18:00 was selected to represent human activity hours.

3. Results

3.1. Spatial distribution of microclimate and thermal comfort

This section analyzes the spatial distribution of pedestrian-level

microclimate and thermal comfort in summer and winter under three planting scenarios: Notree (without tree), Evergreen (with FM trees), and Deciduous (with LS trees).

Figs. 5 and 6 present maps of four primary microclimatic variables (T_a, *RH, WS, MRT*) and two OTC indices (PET, UTCI) at pedestrian height of 1.4 m. These maps compare the three planting scenarios under SVF=0.1, N-S orientation, for summer afternoon (14:00) and winter morning (07:00).

On hot summer afternoon, the air temperatures in the central canyon were lower in both tree-planting scenarios than in the Notree scenario, with cooling effects exceeding 1.5°C. The *RH* maps showed higher values in the central canyon for tree-planting scenarios due to evapotranspiration. For the wind field, narrow ventilation corridors were observed within the N-S oriented street canyons. Compared to the Notree scenario, trees reduced pedestrian-level wind speed by up to 56 %. Cooler zones with low *MRT* values were found across tree zones in the central canyon, demonstrating the cooling effect of tree shading. The combined effects on thermal comfort were illustrated in the PET and UTCI maps. The central canyon, which was hotter in the Notree scenario, was locally cooled by approximately 3 °C in PET and 1 °C in UTCI on average under tree-planting scenarios, indicating substantial heat relief provided by street trees during summer afternoons.

On cold winter morning, air temperature was uniformly distributed across the neighborhood in all three scenarios, ranging from 3 to 5°C, with the evergreen scenario showing slightly lower T_a in the central canyon. The *RH* map for the evergreen scenario showed higher values in the central canyon than Notree and deciduous scenarios. This resulted from evapotranspiration and reduced wind speeds (due to the windbreak effect of evergreen trees), which limited moisture removal. The *WS* map showed lower wind speeds in the evergreen scenario compared to the other two with the spatial maximum reduction of up to 30 % relative to the baseline. This highlights the significant windbreak effect of evergreens in ventilation corridors. MRT maps showed similar distributions to T_a across all three scenarios due to weak solar radiation on early winter morning. Regarding thermal comfort, the evergreen scenario showed a moderate improvement of up to 0.5 °C in PET and 2 °C in UTCI compared to the Notree scenario. In contrast, the deciduous scenario exhibited thermal comfort conditions similar to the Notree scenario. This demonstrates the superiority of evergreen trees for improving winter thermal comfort in deep, narrow canyons with low SVF.

3.2. Diurnal variations of microclimatic and thermal comfort variables

This section further examines the diurnal variations of pedestrian-level microclimatic and thermal comfort variables across the central canyon, using spatial averaged values (Fig. 7). It covers three planting scenarios under both low (SVF=0.2) and high (SVF=0.7) sky view factors, during summer and winter, and for two street orientations (N-S and E-W).

In summer (Fig. 7a), both evergreen and deciduous trees effectively reduced daytime heat stress compared to the Notree scenario, demonstrating their comparable cooling capacity. This is evidenced by their closely aligned diurnal curves for T_a, *RH, MRT*, and the resulting thermal comfort indices PET and UTCI. The cooling effect primarily stemmed from significant attenuation of solar radiation via tree shading and the evapotranspiration during peak daylight hours. Moreover, cooling was more pronounced in E-W oriented canyons than in N-S ones due to the combined effect of tree shading and building shadows, as indicated by larger discrepancies between the Notree and tree-planting scenarios in the E-W scenarios.

In winter (Fig. 7b), both tree species produced a modest reduction in air temperature relative to the Notree scenario across all SVFs and orientations, as their T_a curves are similar. However, a more pronounced divergence appeared in MRT. The persistent canopy of evergreen trees continued to block valuable winter solar radiation in winter, often resulting in lower MRT than under deciduous trees. This effect was particularly detrimental in narrow, low-SVF canyons (SVF=0.2), where the incoming solar radiation was already limited. In contrast, the bare branches of deciduous trees allowed considerable solar penetration, maintaining relatively higher MRT levels on cold, sunny days for both low- and high- SVF canyons. Despite providing weak solar access, evergreens offered markedly superior wind shelter compared to deciduous trees, especially in narrow, low-SVF canyons under N-S orientation. This windbreak effect resulted from the higher LAI and perennial foliage of evergreens, which create a denser, more persistent aerodynamic barrier

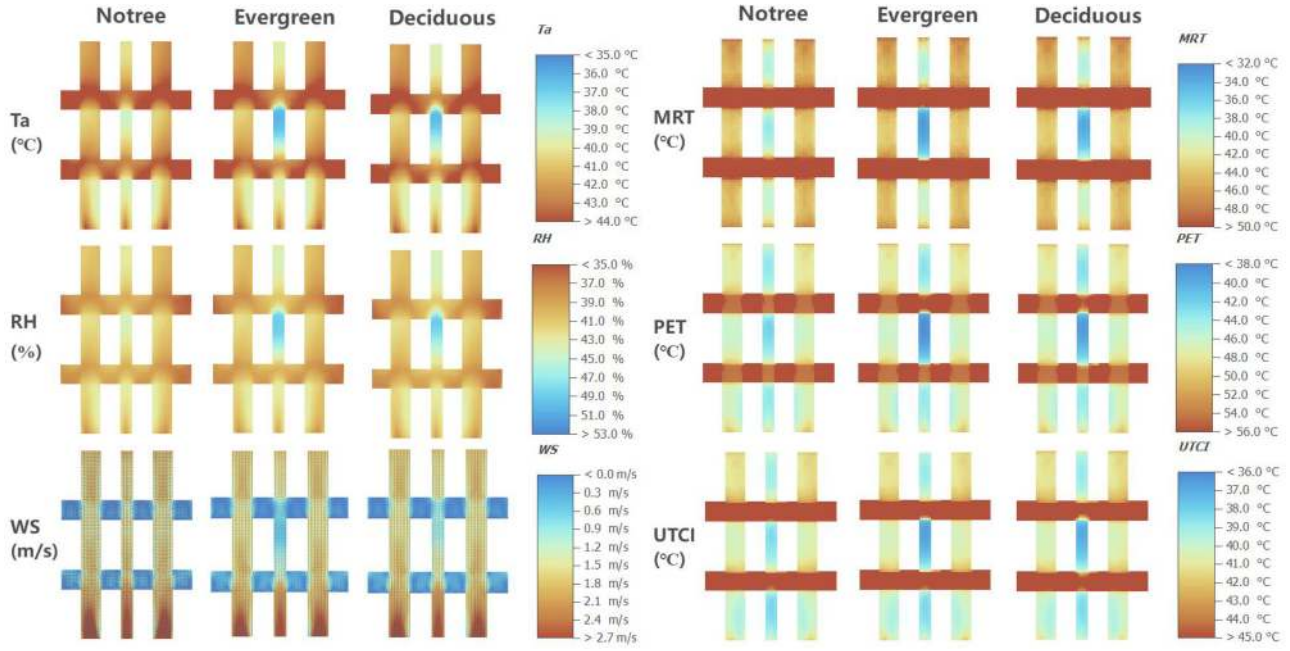


Fig. 5. Maps of pedestrian-level (1.4 m) T_a, *RH, WS, MRT*, PET, UTCI for Notree, evergreen (FM), and deciduous (LS) trees at 14:00 of SVF=0.1, N-S oriented, summer scenario.

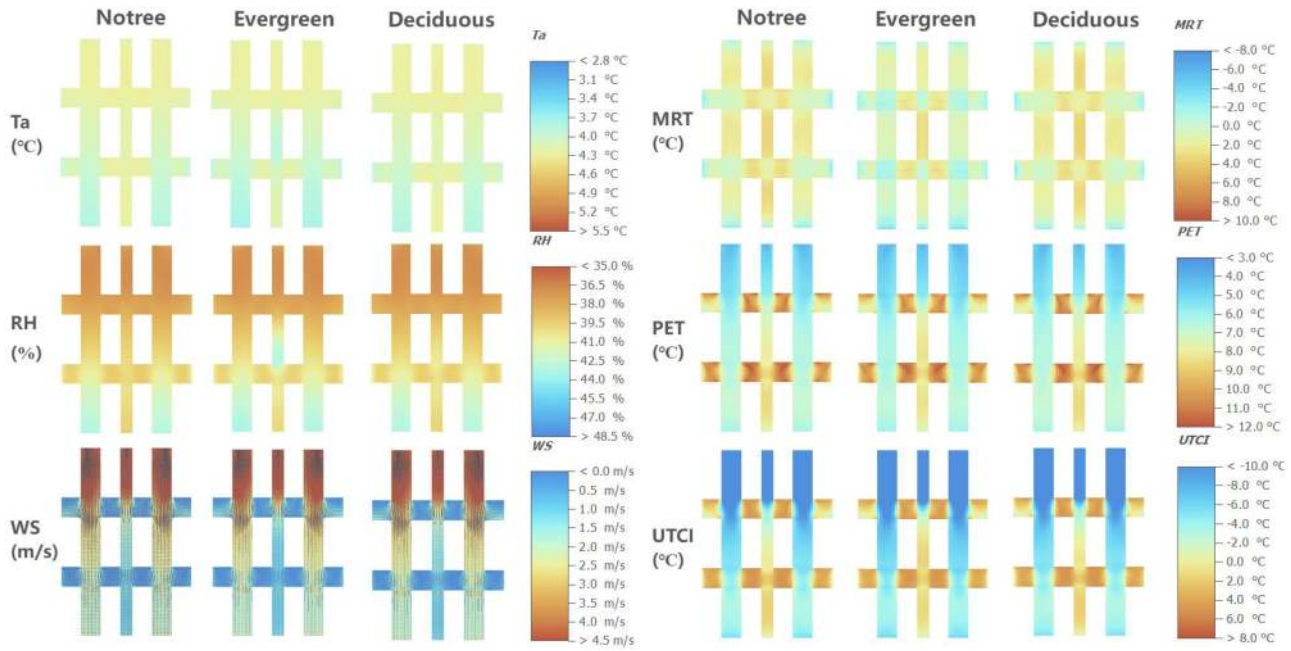


Fig. 6. Maps of pedestrian-level (1.4 m) T_a, *RH, WS, MRT*, PET, UTCI for Notree, evergreen (FM), and deciduous (LS) trees at 07:00 of SVF=0.1, N-S oriented, winter scenario.

during windy coastal winters. Additionally, in those narrow canyons, the Venturi effect can accelerate wind flow when aligned with the prevailing wind direction, yielding a relatively high baseline wind speed (nearly 4 m/s in the Notree scenario). This high reference wind speed enhanced the potential for a measurable wind-reduction effect. However, deciduous trees, after leaf drop, offered less wind reduction under the same conditions.

This fundamental trade-off between solar access and wind shelter provided by evergreen and deciduous trees across SVFs was a key driver of seasonal thermal comfort. Consequently, in low-SVF canyons (SVF=0.2), where wind shielding dominated comfort improvements, PET and UTCI values for evergreens were consistently higher than for the Notree and deciduous scenarios. Conversely, in high-SVF canyons (SVF=0.7), PET and UTCI under deciduous trees closely tracked the Notree scenario and higher than those of evergreen trees during sunlit hours, reflecting their greater solar access in open, shallow canyons.

In summary, both tree species provided similar summer cooling benefits, but their winter performance involved a trade-off that varied with SVF and street orientation. Evergreen trees tended to exacerbate winter cold stress in shallow, high-SVF canyons while offering improved thermal comfort in narrow, low-SVF canyons with N-S orientation due to wind protection. Deciduous trees, by contrast, provided better thermal conditions in open, high-SVF canyons through solar gain but had less impact in closed, low-SVF canyons where wind shelter is more critical.

3.3. Impacts of evergreen and deciduous trees on thermal comfort across SVFs and orientations

This section assesses the overall seasonal impacts of evergreen and deciduous trees on thermal comfort (as calculated by Eq. 3), across SVF (0.1–0.8) and street orientations (N-S and E-W), using the Notree scenario as the reference baseline. The spatial average results for the central canyon are summarized in the boxplots of Fig. 8.

For summer conditions (Fig. 8a), both tree species produced a consistent cooling effect (negative ΔT_a) across all SVFs and orientations, with peak cooling observed at SVF=0.7. At this SVF class, the mean reductions were up to 1.5 °C for ΔT_a, 12.6 °C for ΔMRT, 8.1 °C for ΔPET, and 5.6 °C for ΔUTCI. Critically, the magnitude of ΔT_a differed only minimally between the two tree species, and neither showed a consistent, significant advantage over the other, with the mean absolute cooling difference between evergreen and deciduous was 0.37 °C by PET and 0.56 °C by UTCI (as listed in the statistical summary tables in Appendix F). Through evapotranspiration, both species also increased ambient humidity (positive ΔRH), with a maximum observed increase of approximately 6 % at SVF=0.7. This indicates that, while adding moisture, neither species would substantially exacerbate the already humid local climate. Additionally, both species exhibited windbreak effect. Evergreen trees, with their larger LAI, provided a stronger sheltering effect, as shown by ΔWS values of up to 0.8 m/s in N-S oriented canyon at SVF=0.1. In contrast, the wind-reduction effect was insignificant in E-W oriented canyons, where ΔWS values remained neutral across all SVFs. This disparity is attributed to the sheltering effect of E-W oriented buildings, which lie perpendicular to the prevailing wind.

For winter conditions (Fig. 8b), evergreens maintained a stronger cooling effect (i.e., more negative ΔT_a) than deciduous trees across all SVFs and orientations. This cooling effect was more pronounced in canyons with higher SVFs, reaching a peak reduction of up to 1 °C in T_a, suggesting that evergreen trees are more likely to exacerbate winter cold stress in open, shallow canyons. Notable inter-species differences also emerged in humidity: evergreens caused a marginally greater increase in *RH* relative to deciduous trees, attributable to their perennial foliage sustaining transpiration, whereas leafless deciduous trees provided minimal humidification. Furthermore, the wind-sheltering effect of evergreen trees became even more significant in winter, especially in N-S oriented canyons with lower SVFs, where peak reductions averaged up to 1.5 m/s at SVF=0.2. Leafless deciduous trees, by comparison, showed limited wind shelter capacity across all SVFs.

Moreover, winter *MRT* data revealed a clear divergence between species in solar radiation blocking. The persistent canopy of evergreen trees consistently attenuated incoming solar radiation throughout the day with a maximum reduction of 15.1°C, whereas the leafless canopy of deciduous trees allowed considerable solar penetration with the difference in ΔMRT up to 6.6°C. Consequently, the differing solar access characteristics along with the wind shelter effect of the two species produced distinct impacts on thermal comfort, governed by both tree type and urban geometry.

As evaluated by PET and UTCI, evergreens improved winter comfort primarily through wind shelter. This benefit was most effective in deep,

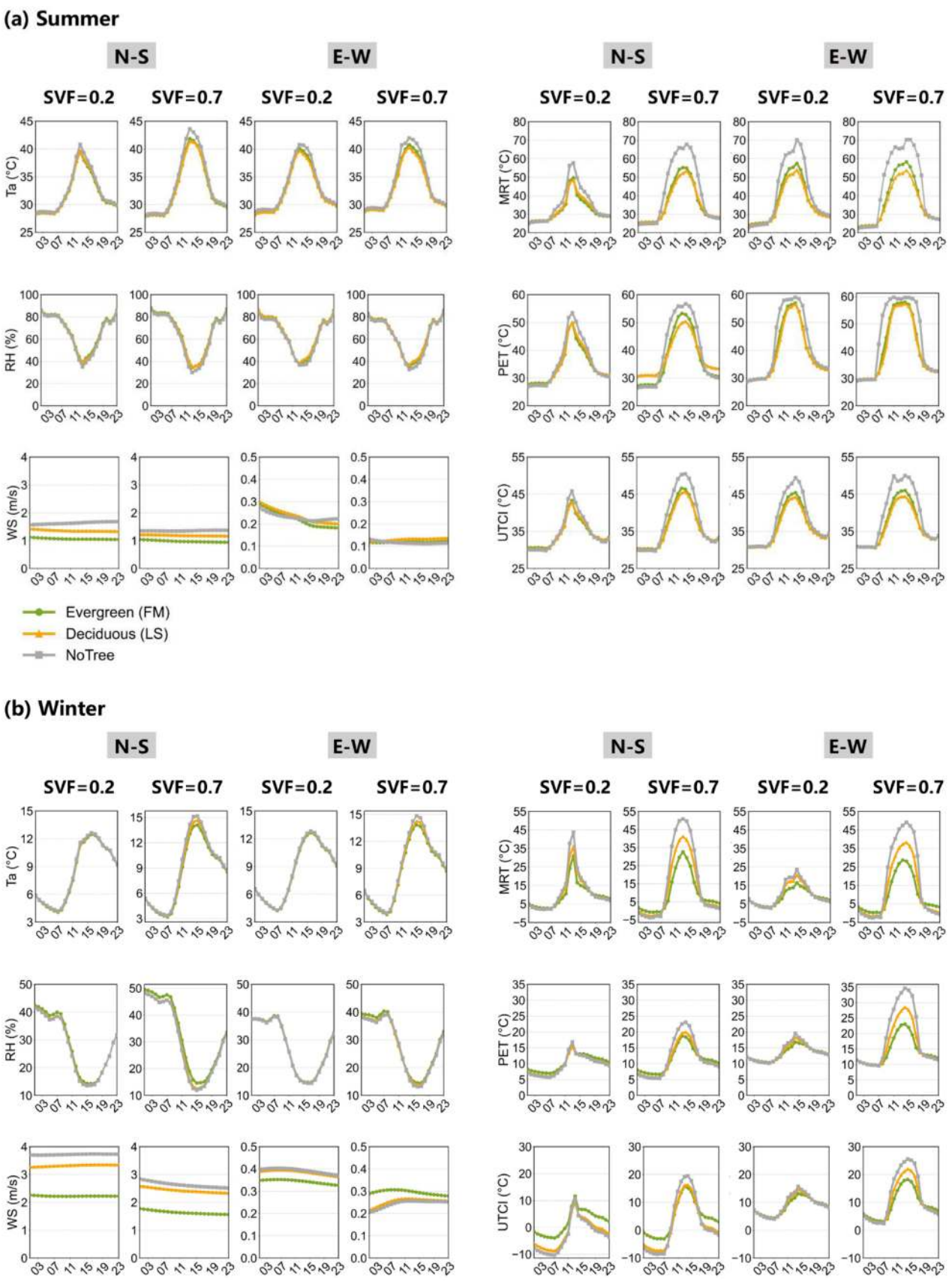


Fig. 7. Diurnal variations (0:00–23:00) of pedestrian-level (1.4 m) T_a, *RH, WS, MRT*, PET, UTCI for Notree, evergreen (FM), and deciduous (LS) trees, under low (SVF=0.2) and high (SVF=0.7) sky view factors with two street orientations during (a) Summer and (b) Winter.

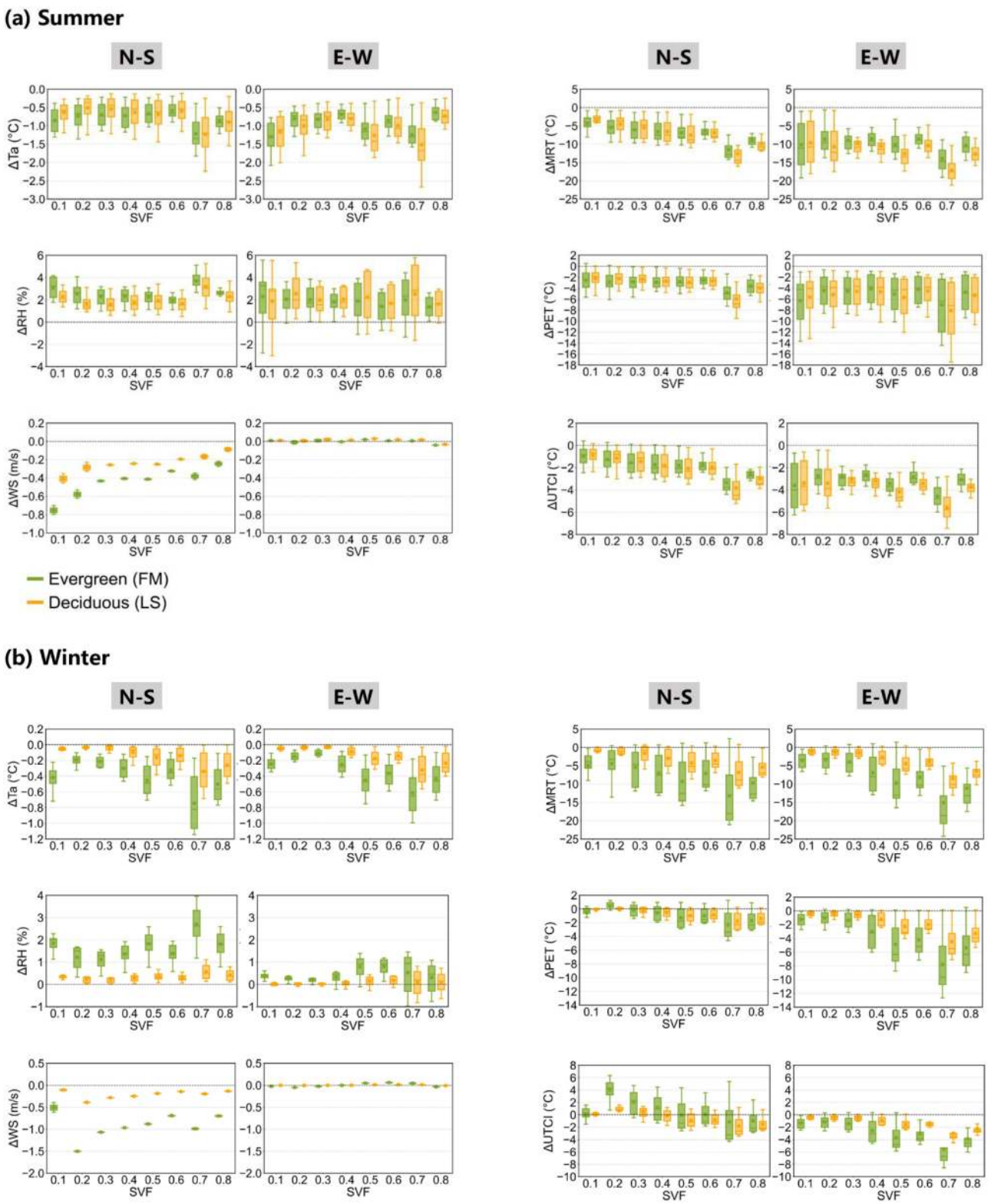


Fig. 8. Boxplots of daytime (07:00–18:00) pedestrian-level (1.4 m) ΔT_a, ΔRH, ΔWS, ΔMRT, ΔPET, ΔUTCI for evergreen (FM) and deciduous (LS) trees across eight SVF canyons and two street orientations during (a) Summer and (b) Winter.

narrow canyons (e.g., SVF=0.1, 0.2, 0.3) with N-S orientation, where ΔPET and ΔUTCI values were positive with maximums of 1.2 °C and 6.3°C. Conversely, deciduous trees enhanced winter comfort mainly by permitting solar gain especially in E-W oriented canyons. Their leafless canopy allowed greater solar penetration into the street canyon, thereby elevating *MRT* and, in turn, PET and UTCI, particularly in open, high-SVF canyons (e.g., SVF=0.7, 0.8), with the peak warming effects of 0.3 °C PET and 1.2 °C UTCI.

4. Discussion

4.1. Seasonal thermal performance of evergreen and deciduous trees

The most salient finding of this study is the pronounced seasonal divergence in the thermal performance of evergreen and deciduous trees, governed by their distinct phenological cycles interacting with the microclimates of urban canyons of varying geometry and orientation.

In summer, both species provided comparable and substantial improvements in thermal comfort, as evidenced by similar reduction in T_a, *MRT*, and consequently, PET and UTCI. The negligible difference in summer cooling performance (mean difference in ΔPET=0.21 °C and ΔUTCI=0.35°C) indicates that for mitigating summer heat stress, the choice between a densely foliated evergreen and a deciduous tree with similar physical traits and LAI is of secondary importance across all canyons regardless SVFs and orientations. The primary mechanism for summer comfort improvement was shading [68], which drastically reduced *MRT* (peak Δ*MRT* of –21°C), with evapotranspiration contributing to a modest additional cooling effect.

In winter, the phenological difference became the dominant factor, creating a critical trade-off that varied with urban geometry, resulting in a balance between wind sheltering and solar access for winter thermal comfort. The evergreen tree acted as a year-round windbreak, proving most thermally beneficial in deep, wind-prone canyons (low-SVF) where mitigating wind chill is the primary objective for winter comfort. However, in open and less windy canyons (high-SVF), it often exacerbated cold stress by blocking valuable winter sunlight, resulting in lower T_a and *MRT*; this negative effect was most detrimental in E-W oriented canyons where solar access was already limited. Conversely, the deciduous tree acted as a seasonally adaptive solar regulator, proving most beneficial in open, sun-exposed canyons (high-SVF) where maximizing solar access is the key to improving thermal comfort on cold, sunny winter days. However, it was less beneficial in windy, shallow, low-SVF canyons. This understanding of the distinct winter roles of evergreen and deciduous trees in subtropical coastal regions differs from conclusions drawn for regions with colder winters [19], warranting caution in transferring planting strategies across climate zones.

It should also be noted that the effect size of urban trees reported in this study are subject to contextual uncertainty arising from model simplifications, idealized canyon geometry, fixed meteorological conditions, and parametric uncertainty. In practice, actual benefits may vary with local climates, urban morphology, and tree species.

4.2. Comparison with prior studies

Table 4 compares the cooling/warming magnitudes from this study with prior studies that examined the influence of trees within urban canyons. Overall, the reviewed literature demonstrates that the thermal effects of trees in such settings are highly context-dependent, varying by climate region, season, tree species, and urban geometry. Summer cooling magnitudes range widely from a 1.2 °C decrease in T_a in Guangzhou to 10 °C reduction in PET in Lhasa, with many studies reporting reductions between 3 to 8 °C in thermal indices (*MRT*, PET, UTCI). Winter effects are more divergent: trees can provide mild cooling (e.g., reductions of 1.3 °C in *MRT* to 4 °C in PET in Lecce and Changsha) or, in some cases, substantial warming (e.g., an increase of 11 °C PET in Lhasa). This contrast underscores the dual role of trees, shading versus solar access, and its seasonal variability across climates.

Results of this study align with established findings that urban trees significantly reduce summer heat stress, with cooling magnitudes (e.g., up to 8 °C in PET) consistent with ranges reported in prior research. The primary divergence lies in winter thermal performance. While limited prior winter studies report either strong winter warming in cold-dry regions or continued cooling in temperate regions, this study reveals a strategy-dependent trade-off for mild winter climates. It demonstrates that evergreen and deciduous trees provide distinct winter benefits in canyons with different openness—through wind shielding and solar access, respectively, a form of seasonal specialization not emphasized in the existing literature. Consequently, it challenges the single-season optimization focus prevent in existing design guidance, highlighting that year-round thermal comfort in subtropical coastal cities requires deliberate species selection and placement tailored to seasonal mechanisms.

4.3. Inconsistency in OTC assessment between PET and UTCI

4.3.1. Different performance in tree evaluation

While both PET and UTCI indices confirmed the overarching seasonal trends, a notable discrepancy emerged in their sensitivity to specific meteorological parameters, particularly in winter.

The PET index appeared to be more strongly influenced by radiative fluxes. This was demonstrated by the significant comfort improvement (less negative ΔPET) provided by deciduous trees in open, high-SVF canyons, where solar penetration was greatest. Year-round measurement of seasonal tree effects in subtropical Hong Kong further confirm

Table 4
Comparison of tree cooling/warming effects within urban canyons: This study versus prior research.

Region (climate type[a])	Time period	Method [b]	Tree [c]	Canopy openness [d]	Cooling/warming magnitude [e]	Ref.
Lhasa, China (BSk)	Summer days (Aug 6–7) Winter day (Dec 26)	O	D	Varying SVF (0.06–0.96)	Summer: –10 °C PET; Winter: +11 °C PET	[69]
Changsha, China (Cfa)	Annual	O & M	E & D	High SVF (≈0.7) *	Winter: –4 °C PET by evergreens	[19]
Lecce, Italy (Csa)	Summer day (Jul 7) Winter day (Dec 3)	O & M	E & D	Moderate SVF (≈0.3, 0.5) *	Summer: –7 °C MRT Winter: –1.3 °C MRT	[70]
Lahti, Finland (Dfb)	Summer day (Jul 17) Winter day (Feb 18)	O & M	E & D	Moderate SVF (≈0.3, 0.5) *	Summer: –3 °C MRT Winter: –1.5 °C MRT	[70]
Guangzhou, China (Cfa)	Shoulder season days (Oct 22, 29; Nov 3, 13)	S	E	Low to moderate SVF (≈0.1–0.4) *	–1.2 °C T_a	[71]
Melbourne, Australia (Cfb)	Summer months (May 2011–Jun 2013)	O	E & D	Moderate to high SVF (0.6–0.8)	–1.5 °C T_a -6 °C UTCI	[72]
Montreal, Canada (Dfb)	Summer heat wave (May 27–29)	M	G	Low & high SVF (≈0.3, 0.8) *	–5 °C UTCI	[38]
Hong Kong (Cwa)	Summer day (Jul 13) Winter day (Feb 5)	M	E & D	Varying SVF (0.1–0.8)	Summer: –8 °C PET, –5 °C UTCI; Winter: +1 °C PET, +6 °C UTCI; –12 °C PET, –8 °C UTCI	This study

[a] Climate types are according to the Köppen-Geiger climate classification [43].
[b] O: Observation; M: Modeling; E: Scaled experiment.
[c] E: Evergreen; D: Deciduous; G: General tree.
[d] SVF values marked with '*' are calculated indirectly from literature data.
[e] Magnitude of cooling/warming effects refers to the temperature difference between the tree and no-tree scenarios. '–' denotes cooling and '+' denotes warming.

the higher weight of radiation in PET calculation [73]. In contrast, the UTCI demonstrated a higher sensitivity to wind speed variations. This was clearly evidenced in the winter N-S scenario, where the wind sheltering effect of evergreen trees in deep, low-SVF canyons resulted in strongly positive mean ΔUTCI values, indicating a warming effect in canyons with SVFs from 0.1 to 0.6. However, PET, under the same conditions, registered only marginally positive or less negative values. The consistently larger interquartile ranges and absolute |Diff| values in Table F2 for UTCI further underscore its heightened responsiveness to wind chill effects, a finding corroborated by sensitivity tests on different meteorological variable for UTCI [67].

4.3.2. *In-depth mechanisms*

This inconsistency likely stems from the fundamental differences in the definition and derivation of the two indices.

- **Definition and derivation of PET**

PET is defined as the air temperature at which, in a typical indoor setting (without wind and solar radiation), the human energy budget would maintain the same core and skin temperatures as in the complex outdoor conditions being assessed [74], i.e., what indoor temperature would feel the same as this current outdoor weather conditions?

PET is derived from the Munich Energy-balance Model for Individuals (MEMI) [74]. This is a sophisticated model of the human body's thermoregulation that calculates the body's energy balance based on: 1) Meteorological inputs: T_a, *RH, WS*, and *MRT*; 2) Personal parameters: Metabolic rate and clothing insulation (which are typically standardized for comparison, e.g., to a person walking at 4 km/h in 0.9 clo level). The model solves the heat balance Eq. for the human body. The output is the PET that would produce the same physiological strain (skin and core temperature) as the outdoor environment. Its derivation through a complete energy balance model gives significant weight to radiant heat exchange, meaning it is highly sensitive to changes in MRT caused by shading or sunlight.

- **Definition and derivation of UTCI**

UTCI is defined as the air temperature of a reference environment that provides the same physiological response for a hypothetical person walking at 4 km/h as the actual outdoor environment [75]. It represents the "isothermal" temperature of a reference condition.

UTCI is derived from a multi-node, dynamic model of human thermoregulation—UTCI-Fiala model. This model simulates the body's physiological responses (e.g., skin blood flow, sweating) to environmental stress [75]. A key outcome of its sophisticated derivation is that it is particularly sensitive to wind speed and humidity variations, as the multi-node model meticulously simulates convective (wind chill) and evaporative (sweating) heat loss processes. This often makes it more responsive to wind variation than PET.

This fundamental difference in their underlying models and the parameter weighting is the root cause of the inconsistency in assessing tree performance in different urban geometry. The inclusions of wind-chill effect for UTCI underscore the role of combined radiant-and-wind effect in shaping winter outdoor thermal comfort, while PET stay stable under such contexts. This finding highlights that the choice of thermal index can influence the interpretation of a tree's comfort benefits, which is crucial for urban planners, suggesting that the assessment of planting strategies should be based on understanding the basis of the index used for proper applications and accurate interpretations.

4.4. *Implications and recommendations for climate-adaptive planting strategies*

There is no doubt that urban trees can provide many benefits to cities in hot summers and thus serve as an efficient design intervention. Results of this study move beyond the generic advice to "plant more trees" and provide a more comprehensive framework for species selection based on specific urban canyon geometries and seasonal priorities from a year-round perspective.

Deciduous trees are generally the optimal choice for maximum annual comfort. They provide near-equivalent cooling benefits to evergreens in summer while permitting beneficial solar gain in winter. This makes them particularly suitable for open, high-SVF canyons (e.g., SVF=0.7) where winter solar access is ample and their positive impact on *MRT* is maximized. Evergreen trees are superior, dedicated windbreaks for targeted wind protection. They should be strategically planted in narrow, deep canyons (low-SVF) with a N-S orientation, where wind tunneling effects (Venturi effect) are most pronounced. The values of PET and UTCI were higher in these scenarios, where mitigating harsh winter winds is a greater priority than gaining solar radiation.

While it is empirically safer and more common to plant evergreen trees in subtropical cities for easier maintenance, a mixed planting strategy is likely more robust. Utilizing deciduous trees along south-facing sidewalks in wide streets maximizes winter sun, while employing evergreens as windbreaks in exposed, windy locations or on the windward side of deep, N-S canyons can create a more comfortable and resilient urban microclimate year-round.

4.5. *Limitations and future works*

While this study offers informative insights, some limitations should be acknowledged and addressed in future research.

First, this study simulated two specific tree species (*Ficus microcarpa* for evergreen, *Lagerstroemia speciose* for deciduous) with fixed physical traits and LAI, using a single-row roadside planting strategy. Future work should investigate a wider range of species and different planting strategies [76,77], including deciduous trees with varying branch structure and evergreens with different canopy densities, as well as configurations like double rows or staggered planting, to create a more comprehensive portfolio for designers. Additionally, the generic urban canyon model was simplified to a fixed canyon consisting of two parallel buildings. Future work should be extended to more complex urban forms, as building morphology can significantly affect the thermal performance of urban trees via building shadows [49,78].

Second, while the Seasonal Leaf Factor (SLF) in ENVI-met provides a practical method to approximate the drastic leaf-on/leaf-off transition of deciduous trees, our modeling approach incorporated two inherent simplifications that warrant further discussion. **(1)** The seasonal shift from summer to winter was simulated solely by modulating LAD via SLF (from 1.0 to 0.2). Although LAD is a primary driver of biophysical processes like radiation interception, transpiration, and wind drag, this approach does not capture full tree phenology. Real seasonal adaptation involves a suite of physiological changes beyond leaf drop, including alterations in leaf optical properties (e.g., chlorophyll content), stem hydraulic conductivity, and root activity [79,80]. These factors collectively influence energy partitioning. For instance, the albedo of a dormant deciduous tree's branch structure differs from that of its summer foliage and from an evergreen, a subtle not captured by a simple LAD reduction. Consequently, while our model effectively captured the gross changes in shading and permeability, it may not fully replicate the subtler radiative and energetic exchanges of a real tree undergoing complex phenological change. This introduced a degree of uncertainty in the simulated effect sizes, particularly for winter radiative exchange and latent heat fluxes. Quantifying this uncertainty would require more advanced phenological parameterization or validation with multi-season field measurement data. **(2)** The soil moisture conditions were held unchanged between summer and winter simulations due to a lack of site-specific, seasonal data to inform this parameter. In reality, soil moisture exhibits strong seasonal dynamics, influenced by precipitation patterns, evaporation rates, and plant water uptake. In our model simulation, the soil moisture profile set likely sustained transpiration

rates at a realistic level in summer. However, in winter, the combination of leafless deciduous trees (SLF=0.2) and unchanged soil moisture could have led to an overestimation of soil evaporation from the tree pits [81], as the model's energy balance at the soil surface was not constrained by the drier conditions typical of the cool season. For evergreen trees, the assumption of unchanged soil moisture and its availability for winter transpiration was a simplification that merits further validation. These issues suggest that the simulated humidity effect of trees (ΔRH) in winter, while minimal, might be slightly overestimated, and the concomitant latent heat effects may not be fully representative.

Third, it is also important to acknowledge the intrinsic limitations of the ENVI-met model itself. As a model with a "black-box" structure, certain aspects of its internal calculations—particularly the CFD formulation, turbulence modeling, and numerical convergence criteria—are not fully user-modifiable. Moreover, the model's reliance on a Cartesian grid limit its precision in representing complex geometries. Therefore, the findings of this study should be interpreted within this context, recognizing that the model provides valuable insights into relative trends and patterns rather than absolute predictions of microclimate variables.

Last, this research focused on physical microclimatic parameters. Future studies should integrate these findings with human subjective perception through field surveys to calibrate the model predictions and validate the thermal comfort indices used [82,83].

5. Conclusions

While the cooling effects of urban trees during summer have been widely explored, their influence on winter thermal comfort, especially in subtropical coastal environments, has received far less attention. This study bridges that gap through parametric simulations using ENVI-met, examining the year-round performance of evergreen (*Ficus microcarpa*) and deciduous (*Lagerstroemia speciose*) trees in eight diverse urban canyons in Hong Kong. By shifting away from a summer-only focus, our work offers a comprehensive view of the benefits and trade-offs these trees bring to pedestrian comfort across seasons.

In summer, both species deliver substantial cooling, primarily through shading that slashes mean radiant temperatures, leading to notable improvements in thermal indices like PET and UTCI, with peak cooling effects of 8 °C in PET and 5 °C in UTCI occurring in moderately open canyons (SVF around 0.7) where shade and geometry strike an ideal balance. The choice between evergreen and deciduous trees matters less here. Winter, however, reveals stark trade-offs shaped by tree behavior and urban form: evergreens excel as wind shields in narrow, N-S oriented canyons with low SVF, curbing chill in windy spots with warming effects up to 1 °C in PET, 6 °C in UTCI, while deciduous trees shine in wider, shallower canyons by allowing vital solar warmth to penetrate with warming magnitudes of up to over 0.3 °C in PET, 1 °C in UTCI.

These patterns hold across thermal comfort metrics, though PET better highlights radiative gains from deciduous trees, and UTCI emphasizes wind protection from evergreens, reminding us to pick indices wisely based on local conditions. Ultimately, our results call for a tailored "right tree, right place, right time" approach over blanket solutions. In subtropical coastal cities, deciduous trees with broad, dense canopies should be the go-to for open areas, boosting winter solar access without skimping on summer relief. Evergreens, meanwhile, are best reserved as targeted windbreaks in deep canyons prone to tunneling effects. A blended planting strategy, mixing both types to suit microlocations, could yield the most resilient urban microclimates.

These insights equip urban planners, landscape architects, and policymakers with practical tools to weave seasonal dynamics and morphology into green infrastructure design, paving the way for cities that stay comfortable and livable year-round in the face of climate challenges.

CRediT authorship contribution statement

Lingye Yao: Writing – review & editing, Writing – original draft, Visualization, Validation, Software, Methodology, Investigation, Formal analysis, Data curation, Conceptualization. **Kevin Lau:** Supervision, Software, Resources, Project administration. **Xiang Zhang:** Writing – review & editing, Software, Methodology, Investigation, Data curation. **Zhixin Liu:** Writing – review & editing, Validation, Supervision, Software, Resources, Methodology, Investigation. **Genyu Xu:** Writing – review & editing, Software, Data curation, Conceptualization. **Kai Gao:** Writing – review & editing, Validation, Software, Methodology, Investigation, Data curation. **Mohammad A. Rahman:** Writing – review & editing, Validation, Software, Methodology. **Edward Ng:** Writing – review & editing, Supervision, Resources, Project administration, Funding acquisition.

Declaration of competing interest

The authors declare that they have no known competing financial interests or personal relationships that could have appeared to influence the work reported in this paper.

Acknowledgement

This work is supported by the Research Impact Fund (No. CUHK R4040-22, entitled '*Increasing the Resilience to the Health Impacts of Extreme Cold Weather on the Older Population under Future Climate Change*') of the Hong Kong Research Grants Council.

Supplementary materials

Supplementary material associated with this article can be found, in the online version, at doi:10.1016/j.buildenv.2026.114471.

Data availability

Data will be made available on request.

References

[1] P. Arias, N. Bellouin, E. Coppola, et al., Climate Change 2021: the physical science basis. Contribution of Working Group I to the Sixth Assessment Report of the Intergovernmental Panel on Climate Change; technical summary, 2021.
[2] M. Alhazmi, J. Anand, The influence of building coverage ratio on building surface reflectivity in reducing building heat release and energy consumption under current and future weather scenarios, Energy Build. 342 (2025), https://doi.org/10.1016/j.enbuild.2025.115889.
[3] X. Yang, L. Yao, M. Li, et al., How heat waves and urban microclimates affect building cooling energy demand? Insights from fifteen eastern Chinese cities, Appl. Energy 384 (2025), https://doi.org/10.1016/j.apenergy.2025.125424.
[4] D.E. Bowler, L. Buyung-Ali, T.M. Knight, et al., Urban greening to cool towns and cities: A systematic review of the empirical evidence, Landsc. Urban Plan. 97 (3) (2010) 147–155, https://doi.org/10.1016/j.landurbplan.2010.05.006.
[5] Z. Liu, K.Y. Cheng, M. Amati, et al., Creating a thermally comfortable city through urban green infrastructure: an international review of greening policies, Urban For. Urban Green. 105 (2025), https://doi.org/10.1016/j.ufug.2025.128713.
[6] N.H. Wong, C.L. Tan, D.D. Kolokotsa, et al., Greenery as a mitigation and adaptation strategy to urban heat, Nat. Rev. Earth Environ. 2 (3) (2021) 166–181, https://doi.org/10.1038/s43017-020-00129-5.
[7] D. Lai, W. Liu, T. Gan, et al., A review of mitigating strategies to improve the thermal environment and thermal comfort in urban outdoor spaces, Sci. Total Env. 661 (2019) 337–353, https://doi.org/10.1016/j.scitotenv.2019.01.062.
[8] Z. Liu, W. Cheng, C.Y. Jim, et al., Heat mitigation benefits of urban green and blue infrastructures: A systematic review of modeling techniques, validation and scenario simulation in ENVI-met V4, Build. Environ. 200 (2021), https://doi.org/10.1016/j.buildenv.2021.107939.
[9] C.Y. Jim, Green-space preservation and allocation for sustainable greening of compact cities, Cities 21 (4) (2004) 311–320, https://doi.org/10.1016/j.cities.2004.04.004.
[10] W. Ouyang, T.E. Morakinyo, C. Ren, et al., Thermal-irradiant performance of green infrastructure typologies: field measurement study in a subtropical climate city, Sci. Total Environ. 764 (2021), https://doi.org/10.1016/j.scitotenv.2020.144635.
[11] Z. Jiang, S. Luo, X. Ma, et al., Analyzing the influence of seasonal and weather changes on thermal effects of a double-skin green façade—A long-term field

measurement, Build. Environ. 271 (2025), https://doi.org/10.1016/j.buildenv.2025.112595.
[12] W. Ouyang, T.E. Morakinyo, Y. Lee, et al., How to quantify the cooling effects of green infrastructure strategies from a spatio-temporal perspective: experience from a parametric study, Landsc. Urban Plan. 237 (2023), https://doi.org/10.1016/j.landurbplan.2023.104808.
[13] A. Middel, N. Chhetri, R. Quay, Urban forestry and cool roofs: assessment of heat mitigation strategies in Phoenix residential neighborhoods, Urban For. Urban Green. 14 (1) (2015) 178–186, https://doi.org/10.1016/j.ufug.2014.09.010.
[14] H. Wu, R. Jin, M. Liu, et al., Investigating the potential of street trees in mitigating pedestrian thermal stress during heatwaves conditions: an empirical study in Guangzhou, Build. Environ. 265 (2024), https://doi.org/10.1016/j.buildenv.2024.111955.
[15] S. Zheng, C. He, J.-M. Guldmann, et al., Heat mitigation benefits of urban trees: A review of mechanisms, modeling, validation and simulation, Forests 14 (12) (2023), https://doi.org/10.3390/f14122280.
[16] M.A. Rahman, C. Hartmann, A. Moser-Reischl, et al., Tree cooling effects and human thermal comfort under contrasting species and sites, Agric. For. Meteorol. 287 (2020), https://doi.org/10.1016/j.agrformet.2020.107947.
[17] H. Li, Y. Zhao, C. Wang, et al., Cooling efficacy of trees across cities is determined by background climate, urban morphology, and tree trait, Commun. Earth Environ. 5 (1) (2024), https://doi.org/10.1038/s43247-024-01908-4.
[18] M.A. Rahman, L.M.F. Stratopoulos, A. Moser-Reischl, et al., Traits of trees for cooling urban heat islands: A meta-analysis, Build. Environ. 170 (2020), https://doi.org/10.1016/j.buildenv.2019.106606.
[19] X. Chen, Z. Li, Z. Wang, et al., The impact of different types of trees on annual thermal comfort in hot summer and cold winter areas, Forests 15 (11) (2024), https://doi.org/10.3390/f15111880.
[20] J. Yang, Y. Zhao, Y. Zou, et al., Improving the thermal comfort of an open space via landscape design: A case study in hot and humid areas, Atmosphere 13 (10) (2022), https://doi.org/10.3390/atmos13101604.
[21] H. Liu, J.Y. Lim, B. Wint Hnin Thet, et al., Evaluating the impact of tree morphologies and planting densities on outdoor thermal comfort in tropical residential precincts in Singapore, Build. Environ. 221 (2022), https://doi.org/10.1016/j.buildenv.2022.109268.
[22] L. Chen, Y. Zhang, J. Han, et al., An investigation of the influence of ground surface properties and shading on outdoor thermal comfort in a high-altitude residential area, Front. Archit. Res. 10 (2) (2021) 432–446, https://doi.org/10.1016/j.foar.2020.12.005.
[23] M.-L. Chong, H.-Y. Yeung, K.-K. Hon, Study of extreme cold surges in Hong Kong, Meteorology 2 (1) (2023) 52–71, https://doi.org/10.3390/meteorology2010004.
[24] H. Baş, İ.T. Doğrusoy, S. Reiter, A proposal of urban coastal pattern for improving pedestrian wind comfort in coastal cities, J. Build. Phys. 47 (2) (2023) 151–181, https://doi.org/10.1177/17442591231177429.
[25] J. Wu, Y. Wang, S. Li, et al., Quantitative study on the effects of street geometries and tree configurations on the outdoor thermal environment, Energies 17 (9) (2024), https://doi.org/10.3390/en17092223.
[26] J.-Y. Deng, N.H. Wong, Impact of urban canyon geometries on outdoor thermal comfort in central business districts, Sustain. Cities Soc. 53 (2020), https://doi.org/10.1016/j.scs.2019.101966.
[27] S. Yin, F. Wang, Y. Xiao, et al., Comparing cooling efficiency of shading strategies for pedestrian thermal comfort in street canyons of traditional shophouse neighbourhoods in Guangzhou, China, Urban Clim. (2022) 43, https://doi.org/10.1016/j.uclim.2022.101165.
[28] C. Miao, S. Yu, Y. Hu, et al., Review of methods used to estimate the sky view factor in urban street canyons, Build. Environ. 168 (2020), https://doi.org/10.1016/j.buildenv.2019.106497.
[29] I. Watson, G. Johnson, Graphical estimation of sky view-factors in urban environments, J. Climatol. 7 (2) (1987) 193–197.
[30] M.K. Svensson, Sky view factor analysis – implications for urban air temperature differences, Meteorol. Appl. 11 (3) (2006) 201–211, https://doi.org/10.1017/s1350482704001288.
[31] G. Baghaeipoor, N. Nasrollahi, The effect of Sky view factor on air temperature in high-rise urban residential environments, J. Daylighting 6 (2) (2019) 42–51, https://doi.org/10.15627/jd.2019.6.
[32] Z. Tan, K.K.-L. Lau, E. Ng, Urban tree design approaches for mitigating daytime urban heat island effects in a high-density urban environment, Energy Build. 114 (2016) 265–274, https://doi.org/10.1016/j.enbuild.2015.06.031.
[33] T.E. Morakinyo, W. Ouyang, K.K. Lau, et al., Right tree, right place (urban canyon): tree species selection approach for optimum urban heat mitigation - development and evaluation, Sci. Total Env. 719 (2020) 137461, https://doi.org/10.1016/j.scitotenv.2020.137461.
[34] Z. Tan, K.K.-L. Lau, E. Ng, Planning strategies for roadside tree planting and outdoor comfort enhancement in subtropical high-density urban areas, Build. Environ. 120 (2017) 93–109, https://doi.org/10.1016/j.buildenv.2017.05.017.
[35] S. Fellini, M. Marro, A.V. Del Ponte, et al., High resolution wind-tunnel investigation about the effect of street trees on pollutant concentration and street canyon ventilation, Build. Environ. 226 (2022), https://doi.org/10.1016/j.buildenv.2022.109763.
[36] Y. Zhao, H. Li, R. Bardhan, et al., The time-evolving impact of tree size on nighttime street canyon microclimate: wind tunnel modeling of aerodynamic effects and heat removal, Urban Clim. 49 (2023), https://doi.org/10.1016/j.uclim.2023.101528.
[37] A. Kubilay, A. Rubin, D. Derome, et al., Wind-comfort assessment in cities undergoing densification with high-rise buildings remediated by urban trees, J. Wind Eng. Ind. Aerodyn. 249 (2024), https://doi.org/10.1016/j.jweia.2024.105721.
[38] C. Nevers, J. Carmeliet, D. Strebel, et al., Understanding cooling potential of urban trees in a typical North America neighborhood, Build. Environ. 282 (2025), https://doi.org/10.1016/j.buildenv.2025.113303.
[39] Y. Yang, E. Gatto, Z. Gao, et al., The "plant evaluation model" for the assessment of the impact of vegetation on outdoor microclimate in the urban environment, Build. Environ. 159 (2019), https://doi.org/10.1016/j.buildenv.2019.05.029.
[40] S. Rahimi, M. Alvarez, U. Berardi, et al., Coupled urban physics in microclimate modeling: validating and enhancing simulation tools, Build. Environ. 285 (2025), https://doi.org/10.1016/j.buildenv.2025.113637.
[41] Z. Liu, K.Y. Cheng, T. Sinsel, et al., Modeling microclimatic effects of trees and green roofs/façades in ENVI-met: sensitivity tests and proposed model library, Build. Environ. 244 (2023), https://doi.org/10.1016/j.buildenv.2023.110759.
[42] ENVI-met Model architecture https://envi-met.info/doku.php?id=intro:modelconcept, 2025.
[43] H.E. Beck, N.E. Zimmermann, T.R. McVicar, et al., Present and future Koppen-Geiger climate classification maps at 1-km resolution, Sci. Data 5 (2018) 180214, https://doi.org/10.1038/sdata.2018.214.
[44] HKO, Climate of Hong Kong. https://www.hko.gov.hk/en/cis/climahk.htm. 2025).
[45] G. Xu, H. Zhao, J. Li, et al., Thermal environment control units for multi-objective urban optimization in territorial spatial planning, Sustain. Cities Soc. 119 (2025), https://doi.org/10.1016/j.scs.2024.106119.
[46] K. Gao, J. Feng, L. Yao, et al., Ensuring accurate microclimate research: how to select representative meteorological data of local climate in microclimate studies, Build. Environ. 267 (2025), https://doi.org/10.1016/j.buildenv.2024.112166.
[47] ENVI-met, Enhance urban green spaces with ENVI-met: optimizing vegetation efficiency, resilience, and safety, 2025. https://envi-met.com/fields-of-analysis/trees-and-vegetation/.
[48] Z. Liu, S. Zheng, L. Zhao, Evaluation of the ENVI-met vegetation model of four common tree species in a subtropical hot-humid area, Atmosphere 9 (5) (2018), https://doi.org/10.3390/atmos9050198.
[49] Q. Wang, L.L.H. Peng, W. Jiang, et al., Urban form affects the cool island effect of urban greenery via building shadows, Build. Environ. 254 (2024), https://doi.org/10.1016/j.buildenv.2024.111398.
[50] X. Zhang, P. Ren, L.-Y. Yao, et al., Investigating tree shading and thermal variations in a subtropical zone: single tree to urban squares, Build. Environ. 283 (2025), https://doi.org/10.1016/j.buildenv.2025.113408.
[51] H. Chen, R. Liu, Y. Zhang, The impact of vegetation canopy on the outdoor thermal environment in cold winter and spring, Sustainability 15 (17) (2023), https://doi.org/10.3390/su151712818.
[52] P.J. Crank, D.J. Sailor, G. Ban-Weiss, et al., Evaluating the ENVI-met microscale model for suitability in analysis of targeted urban heat mitigation strategies, Urban Clim. 26 (2018) 188–197, https://doi.org/10.1016/j.uclim.2018.09.002.
[53] T. Sinsel, H. Simon, W. Ouyang, et al., Implementation and evaluation of mean radiant temperature schemes in the microclimate model ENVI-met, Urban Clim. (2022) 45, https://doi.org/10.1016/j.uclim.2022.101279.
[54] E. Ng, L. Chen, Y. Wang, et al., A study on the cooling effects of greening in a high-density city: an experience from Hong Kong, Build. Environ. 47 (2012) 256–271, https://doi.org/10.1016/j.buildenv.2011.07.014.
[55] T.R. Oke, Street design and urban canopy layer climate, Energy Build. 11 (1-3) (1988) 103–113, https://doi.org/10.1016/0378-7788(88)90026-6.
[56] D. Bureau, in: L.a.T.M.S. Greening (Ed.), Street Tree Selection Guide: The Top 20 Common Urban Trees, 2025.
[57] Y. Xing, P. Brimblecombe, S. Wang, et al., Tree distribution, morphology and modelled air pollution in urban parks of Hong Kong, J. Env. Manage 248 (2019) 109304, https://doi.org/10.1016/j.jenvman.2019.109304.
[58] B. Lalic, D.T. Mihailovic, An empirical relation describing leaf-area density inside the forest for environmental modeling, J. Appl. Meteorol. 43 (4) (2004) 641–645, https://doi.org/10.1175/1520-0450(2004)043<0641:Aerdld>2.0.Co;2.
[59] E. Burton, Measuring urban compactness in UK towns and cities, Environ. Plan. B: Plan. Des. 29 (2) (2002) 219–250.
[60] X. Yang, L. Zhao, M. Bruse, et al., Evaluation of a microclimate model for predicting the thermal behavior of different ground surfaces, Build. Environ. 60 (2013) 93–104, https://doi.org/10.1016/j.buildenv.2012.11.008.
[61] J. Yang, M.S. Wong, H.C. Ho, et al., A semi-empirical method for estimating complete surface temperature from radiometric surface temperature, a study in Hong Kong city, Remote Sens. Environ. 237 (2020), https://doi.org/10.1016/j.rse.2019.111540.
[62] W. Ouyang, T. Sinsel, H. Simon, et al., Evaluating the thermal-radiative performance of ENVI-met model for green infrastructure typologies: experience from a subtropical climate, Build. Environ. 207 (2022), https://doi.org/10.1016/j.buildenv.2021.108427.
[63] X. Zhong, L. Zhao, P. Ren, et al., The role of UAV-derived multimodal images in outdoor thermal comfort observation, evaluation, and improvement: A case study in Guangzhou, Sustain. Cities Soc. 131 (2025), https://doi.org/10.1016/j.scs.2025.106723.
[64] N. Narimani, A. Karimi, R.D. Brown, Effects of street orientation and tree species thermal comfort within urban canyons in a hot, dry climate, Ecol. Inform. 69 (2022), https://doi.org/10.1016/j.ecoinf.2022.101671.
[65] P.K. Cheung, C.Y. Jim, Comparing the cooling effects of a tree and a concrete shelter using PET and UTCI, Build. Environ. 130 (2018) 49–61, https://doi.org/10.1016/j.buildenv.2017.12.013.
[66] W. Ouyang, T.E. Morakinyo, C. Ren, et al., The cooling efficiency of variable greenery coverage ratios in different urban densities: A study in a subtropical

climate, Build. Environ. 174 (2020), https://doi.org/10.1016/j.buildenv.2020.106772.
[67] S. Provencal, O. Bergeron, R. Leduc, et al., Thermal comfort in Quebec City, Canada: sensitivity analysis of the UTCI and other popular thermal comfort indices in a mid-latitude continental city, Int. J. Biometeorol. 60 (4) (2016) 591–603, https://doi.org/10.1007/s00484-015-1054-2.
[68] X. Zhang, L. Zhao, L. Yao, et al., Investigating the micro-scale thermal effects of natural underlying surfaces on adjacent spaces in a subtropical zone with an optimized method, Build. Environ. 222 (2022), https://doi.org/10.1016/j.buildenv.2022.109382.
[69] S. Jayasinghe, V. Jayasooriya, S.M. Dassanayake, et al., Effects of street tree configuration and placement on roadside thermal environment within a tropical urban canyon, Int. J. Biometeorol. 68 (6) (2024) 1133–1142, https://doi.org/10.1007/s00484-024-02653-1.
[70] E. Gatto, R. Buccolieri, E. Aarrevaara, et al., Impact of urban vegetation on outdoor thermal comfort: comparison between a Mediterranean City (Lecce, Italy) and a Northern European City (Lahti, Finland), Forests 11 (2) (2020), https://doi.org/10.3390/f11020228.
[71] T. Chen, H. Yang, G. Chen, et al., Integrated impacts of tree planting and aspect ratios on thermal environment in street canyons by scaled outdoor experiments, Sci. Total Env. 764 (2021) 142920, https://doi.org/10.1016/j.scitotenv.2020.142920.
[72] A.M. Coutts, E.C. White, N.J. Tapper, et al., Temperature and human thermal comfort effects of street trees across three contrasting street canyon environments, Theor. Appl. Climatol. 124 (1-2) (2015) 55–68, https://doi.org/10.1007/s00704-015-1409-y.
[73] P.K. Cheung, C.K. Fung, C.Y. Jim, Seasonal and meteorological effects on the cooling magnitude of trees in subtropical climate, Build. Environ. 177 (2020) 106911, https://doi.org/10.1016/j.buildenv.2020.106911.
[74] P. Höppe, The physiological equivalent temperature–a universal index for the biometeorological assessment of the thermal environment, Int. J. Biometeorol. 43 (2) (1999) 71–75, https://doi.org/10.1007/s004840050118.
[75] P. Bröde, D. Fiala, K. Błażejczyk, et al., Deriving the operational procedure for the Universal Thermal Climate Index (UTCI), Int. J. Biometeorol. 56 (3) (2012) 481–494, https://doi.org/10.1007/s00484-011-0454-1.
[76] T.E. Morakinyo, Y.F. Lam, Simulation study on the impact of tree-configuration, planting pattern and wind condition on street-canyon's micro-climate and thermal comfort, Build. Environ. 103 (2016) 262–275, https://doi.org/10.1016/j.buildenv.2016.04.025.
[77] M.A. Rahman, D. Armson, A.R. Ennos, A comparison of the growth and cooling effectiveness of five commonly planted urban tree species, Urban Ecosyst. 18 (2) (2014) 371–389, https://doi.org/10.1007/s11252-014-0407-7.
[78] T.E. Morakinyo, L. Kong, K.K.-L. Lau, et al., A study on the impact of shadow-cast and tree species on in-canyon and neighborhood's thermal comfort, Build. Environ. 115 (2017) 1–17, https://doi.org/10.1016/j.buildenv.2017.01.005.
[79] A. Ammar, I.B.E.N. Aissa, M. Mars, et al., Seasonal variation of fig tree (Ficus carica L.) physiological characteristics reveals its adaptation performance, S. Afr. J. Bot. 132 (2020) 30–37, https://doi.org/10.1016/j.sajb.2020.04.020.
[80] A. Moser-Reischl, M.A. Rahman, S. Pauleit, et al., Growth patterns and effects of urban micro-climate on two physiologically contrasting urban tree species, Landsc. Urban Plan. 183 (2019) 88–99, https://doi.org/10.1016/j.landurbplan.2018.11.004.
[81] S.E. Gill, M.A. Rahman, J.F. Handley, et al., Modelling water stress to urban amenity grass in Manchester UK under climate change and its potential impacts in reducing urban cooling, Urban For. Urban Green. 12 (3) (2013) 350–358, https://doi.org/10.1016/j.ufug.2013.03.005.
[82] H. Wu, H. Zhao, Z. Nie, et al., Pedestrians thermal responses under variable exposure conditions during heatwaves, Sustain. Cities Soc. 131 (2025) 106703, https://doi.org/10.1016/j.scs.2025.106703.
[83] W.-A. Chen, P.-L. Fang, R.-L. Hwang, Calibrating the UTCI scale for hot and humid climates through comprehensive year-round field surveys to improve the adaptability, Urban Clim. 59 (2025), https://doi.org/10.1016/j.uclim.2024.102267.